Electrochemical and Solid-State Letters, **11** (12) P17-P19 (2008)
1099-0062/2008/11(12)/P17/3/$23.00 © The Electrochemical Society

Structure and Dynamics of Ge in the Si–SiO_2 System: Implications for Oxide-Embedded Ge Nanoparticle Formation

Decai Yu and Gyeong S. Hwang[z]

Department of Chemical Engineering, University of Texas at Austin, Austin, Texas 78712, USA

Using gradient corrected periodic density functional theory calculations, we have investigated the structure, energetics, bonding, and diffusion of Ge in bulk α-quartz and amorphous a-SiO_2 matrices as well as at the Si(001)/a-SiO_2 interface. Our calculations show that Ge atoms undergo migration in a-SiO_2 with a moderate barrier (<2.5 eV) and prefer to remain in the Si part near the Si(001)/a-SiO_2 interface via site exchange reaction with Si lattice atoms, while the kicked-out Si atoms are preferentially incorporated into the a-SiO_2 matrix. We also discuss implications of the Ge–Si exchange process for Ge nanoparticle formation in an oxide matrix.
 [DOI: 10.1149/1.2978960]

Manuscript submitted July 3, 2008; revised manuscript received August 15, 2008. Published September 17, 2008.

Over recent years there has been a growing effort[1-5] to explore oxide embedded Ge nanocrystals (NCs) because of their promising applications in electronic and optoelectronic devices. The unique properties of NCs are often a strong function of particle size and crystallinity, particle size distribution, particle density, and positioning. Therefore, the ability to control the NC characteristics is crucial for their successful application. However, even the underlying mechanism of Ge NC nucleation and growth is ambiguous, despite its importance in guiding how to achieve the desired properties. One of the first steps to establish the complex NC growth kinetics is to better understand the behavior of Ge in the Si/SiO_2 system, which has been rarely studied at the atomistic level.

In this paper, we present the structure and diffusion of Ge in the Si–SiO_2 system based on gradient corrected density functional theory calculations. We first determine the structure, bonding, and diffusion mechanism of Ge in crystalline (α-quartz) and amorphous SiO_2 (a-SiO_2), and then evaluate the structure and energetics of Ge and Si atoms at the Si(001)/a-SiO_2 interface. Based on the calculation results, we also discuss a possible mechanism contributing to Ge NC formation in the oxide matrix.

Calculation Methods

Bulk crystalline SiO_2 (α-quartz) is modeled using a 72 atom supercell with lattice constants of a = 4.917 Å and c = 5.430 Å (see Fig. 1a). Due to flexible Si–O–Si linkages, the supercell size appears to be sufficient for describing the structure and diffusion of an inserted Si (or Ge) atom with no significant interaction with its periodic images.[6,7] We constructed the structure of amorphous SiO_2 (a-SiO_2), which contains 24 SiO_2 units within the continuous random network (CRN) model with fourfold-coordinated Si and twofold-coordinated O.[6,7] Starting with randomly distributed 24 Si and 48 O atoms in the given supercell with a fixed experimental density of 2.2 g/cm^3, the oxide system was relaxed via a sequence of bond transpositions using the Metropolis Monte Carlo (MMC) method based on Keating-like interatomic potentials. The a-SiO_2 structure (Fig. 1b) was further refined using density functional theory (DFT) calculations (as detailed below). The average Si–O–Si bond angle and the bond angle deviation of the a-SiO_2 model structure are ≈136° and ≈15°, respectively, in good agreement with experimental measurements.[8] The CRN–MMC calculation was also performed to construct the Si(001)/a-SiO_2 interface structure. Starting with a periodic Si/c-SiO_2 structure (which contains nine c-Si atomic layers and four c-SiO_2 layers), the a-SiO_2 part was created via a large number of bond transpositions while the c-Si part was fixed. As illustrated in Fig. 1c, the lateral size of the simulation cell corresponds to the (2×2) cell of Si, with a Si lattice constant of 5.431 Å. The CRN–MMC approach has successfully been used to generate the Si(001)/a-SiO_2 interface.[6]

All atomic structures and energies reported herein were calculated using a plane-wave basis set pseudopotential method within the generalized gradient approximation (PW91)[9] to DFT, as implemented in the well-established Vienna ab initio Simulation Package.[10] Vanderbilt-type ultrasoft pseudopotentials[11] were used for core–electron interactions. A plane-wave cutoff energy of 300 eV was used. The convergence of atomic configurations and relative energies with respect to the plane-wave cutoff energy was carefully checked by increasing the cutoff energy to 450 eV, but the variation of relative energies turns out to be insignificant (<0.1 eV), with unnoticeable changes in atomic structures. The Brillouin zone sampling was performed using a $(2 \times 2 \times 2)$ and $(2 \times 2 \times 1)$ mesh of k-points in the scheme of Monkhorst–Pack[12] for the bulk SiO_2 and the Si(001)/a-SiO_2 interface models, respectively. All atoms were fully relaxed using the conjugate gradient method until residual forces on constituent atoms became smaller than 0.02 eV/Å. We calculated diffusion pathways and barriers using the nudged elastic band method,[13,14] which allows a systematic search for the minimum energy path between two local minima with no prior knowledge of the potential energy surface. For a few selected

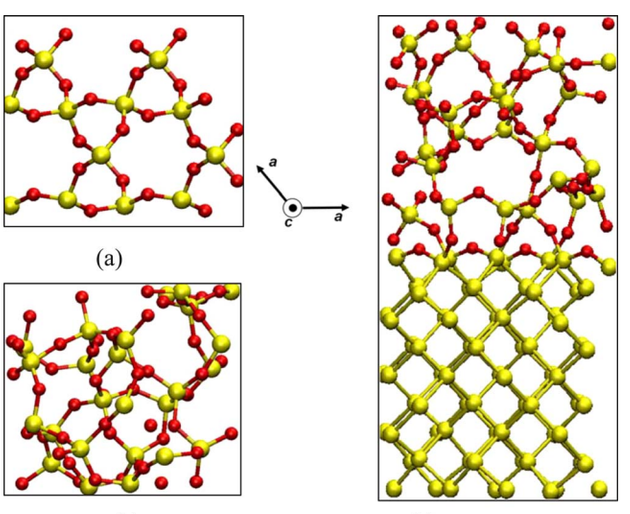

Figure 1. (Color online) Model structures of (a) α-quartz, (b) a-SiO_2, and (c) Si(001)/a-SiO_2 interface. Darker gray (red) and gray (yellow) balls represent oxygen and silicon atoms, respectively. The α-quartz model is shown from the perspective of c-axis.

[z] E-mail: gshwang@che.utexas.edu

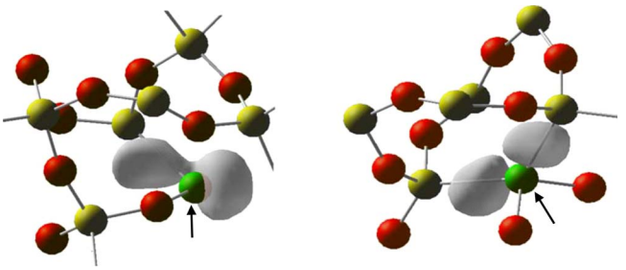

Figure 2. (Color online) Structure and isosurfaces of electron localization functions (at the value of 0.82) of the (a) BC and (b) FC states of Ge in α-quartz. Darker gray (red), dark gray (green, as also indicated), and gray (yellow) balls represent oxygen, germanium, and silicon atoms, respectively.

cases, we analyzed bonding mechanisms using the electron localization function (ELF) as proposed by Becke and Edgecombe.[15] The ELF represents the probability of electron pair localization, and can take on values ranging from 0 to 1, where ELF = 1 corresponds to perfect electron pair localization and ELF = 1/2 corresponds to the probability as in a homogeneous electron gas.

Results and Discussion

α-quartz and a-SiO$_2$.— We first examined the structure and diffusion of Ge in bulk SiO_2. In α-quartz, the most favorable site for neutral Ge is the Si^{4+}–O bond center (BC), as shown in Fig. 2a. The divalent Ge atom may convert to a fourfold coordinated (FC) state where the Ge atom is bonded to neighboring two Si and two O lattice atoms by breaking two original Si–O bonds (see Fig. 2b). The FC state turns out to be 0.8 eV less favorable than the BC state, unlike the Si case where the former is about 0.6 eV more stable than the latter. We attribute this to the weaker Ge–O bond strength, relative to the Si–O case. The bond dissociation energies of SiO_2 and GeO_2 have been reported to be 800 and 659 kJ/mol, respectively.[16]

α-quartz has two unequal Si–O bonds with bond lengths of 1.62 and 1.61 Å, but corresponding Ge BC states (indicated as BC_I and BC_{II}, respectively, hereafter) are nearly degenerate. As illustrated in Fig. 2, the inserted Ge atom forms a covalent-like bond with a Si atom, and an ionic-like bond with an O atom, with large lattice distortion. For the BC state, a lone pair is localized on the Ge atom.

In α-quartz, Ge diffusion appears to occur via a series of hops between adjacent BC sites. The barriers for $BC_I \leftrightarrow BC_I$, $BC_{II} \leftrightarrow BC_{II}$, and $BC_I \leftrightarrow BC_{II}$ hops (over a lattice Si atom) are predicted to be 1.4, 1.1, and 1.7 eV, respectively. A series of $BC_I \leftrightarrow BC_I$ and/or $BC_{II} \leftrightarrow BC_{II}$ hops leads to migration along the *c*-axis, whereas Ge may migrate along the *a*-axis via $BC_I \leftrightarrow BC_{II}$ hopping. Our calculation also predicts a barrier of 1.3 eV for the site exchange between adjacent Ge and O atoms.

Next, we looked at the relative stability between the BC and FC states in a-SiO_2. Because there is a significant site-to-site variation in the energetics of BC and FC, depending on the local strain environment,[7] we first evaluated the difference of their bond energies using model clusters (which yield the least strain energy). That is, $(OH)_3Si–Ge–O–Si(OH)_3 + (OH)_3Si–O–Si(OH)_3 \rightarrow [Si(OH)_3]_2–Ge–[O–Si(OH)_3]_2$, as shown in Fig. 3. Note that the reaction assumes the formation of new Si–Ge and Ge–O bonds while breaking one Si–O bond, mimicking the BC → FC transformation. For the ideal strain-free case, the BC → FC conversion is predicted to be exothermic by 0.3 eV, far smaller than 1.8 eV for the case of Si.[7] Given the small bond energy difference and the fact that the FC state usually yields a larger degree of strain, one could expect that the BC state would be prevailing rather than the FC state in the a-SiO_2 matrix. According to our periodic supercell calculations, in bulk a-SiO_2 indeed the BC state appears favored over the FC state at most locations considered.

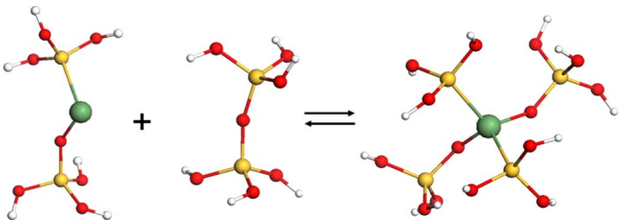

Figure 3. (Color online) Cluster models used to examine the relative stability of the BC and FC structures of Ge in a-SiO_2 where the structures are assumed to be fully relaxed. Large dark gray (green), gray (yellow), small darker gray (red), and small white balls indicate Ge, Si, O, and H atoms, respectively.

Considering that the BC state is dominant in a-SiO_2, Ge diffusion can be expected to occur mainly via a series of BC ↔ BC hops, like in α-quartz. Our supercell calculations predict the corresponding diffusion barrier to be 1.8 ± 0.6 eV, depending on the local strain condition, which is far smaller than 4.7 ± 0.3 eV as predicted for Si self-diffusion in a-SiO_2.[7] Here, to achieve good statistics we considered 25 different locations using five different (72 atom) a-SiO_2 supercells. The moderate barrier implies an ease of Ge diffusion at elevated temperatures, consistent with recent experiments demonstrating that Ge can be quite mobile in SiO_2.[17]

Si(001)/a-SiO$_2$ interface.— As shown in Fig. 4, we identified three stable configurations of interstitial Ge at the Si(001)/a-SiO_2 interface, including: (a) Si^{2+}–Si^0 BC, where the Ge atom is bonded to an interface Si^{2+} atom and a sublayer Si^0 atom by breaking a Si^{2+}–Si^0 back bond, (b) Si^{2+}–O BC, where the Ge forms bonds with Si^{2+} and O atoms while breaking an interface Si^{2+}–O bond, and (c) (111)-split, where the Ge atom and an interface Si^{2+} atom are aligned in the (111) direction while sharing a lattice site.

At the Si/SiO_2 interface, the Ge formation energy significantly varies from site to site due to the disordered a-SiO_2 network, which causes a variation in the local strain along the interface. For the model structure considered, the energy differences between the most and least stable Si^{2+}–Si^0 BC, Si^{2+}–O BC, and (111)-split states are 0.8, 1.6, and 0.7 eV, respectively. Among more than 10 different sites for each state, the most stable Si^{2+}–Si^0 BC state is 0.1 and 0.4 eV more favorable than the most stable Si^{2+}–O and (111)-split states, respectively, and on average 0.2 and 0.5 eV more favorable. This is not surprising considering the higher bond energy of Si–O than Ge–O as well as the more flexible a-SiO_2 network than c-Si. At the (111)-split state the Ge and Si^{2+} atoms exhibit sp^3 and sp^2 hybridization, respectively, indicating charge transfer from the Si^{2+} to the Ge atoms.

Our DFT calculations show that the interstitial Ge at the Si/SiO_2 interface is more stable than in bulk Si. The most stable Si^{2+}–Si^0, Si^{2+}–O BC, and (111)-split states are predicted to be 1.0, 0.9, and 0.6 eV more favorable, respectively, than the ⟨110⟩-split state in the middle of the Si layer (where the interface effect becomes insignificant.[6]) Note that in c-Si the ⟨110⟩-split state is most favor-

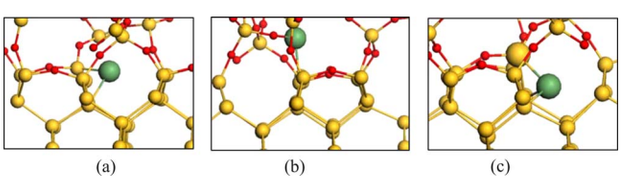

Figure 4. (Color online) Optimized configurations for interstitial Ge at the Si(001)/a-SiO_2 interface. (a) Si–Si BC (b) (111)-split, and (c) Si–O BC. Big dark gray (green), gray (yellow), and small darker gray (red) indicate Ge, Si, and O atoms, respectively.

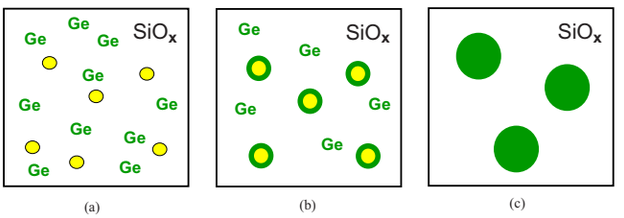

Figure 5. (Color online) Schematic illustration of a possible mechanism contributing to the formation of Ge particles in Si–Ge–O system. (a) Si-rich region formation in the oxide matrix via Si–SiO_2 phase separation, (b) diffusion of Ge atoms to the Si-rich part, and undergo site exchange with lattice Si atoms, while the kicked-out Si atoms are incorporated into the oxide matrix, (c) Ge particle growth via continued Si–SiO_2 phase separation and Ge–Si site exchange in Si-rich regions. Gray (yellow) and darker gray (green) regions represent Si and Ge parts, respectively.

able for a neutral Ge interstitial, while the Si–Si BC and (111)-split states are highly unlikely. We also find that the Si^{4+}–O BC state in a-SiO_2 is as favorable as the interface Si^{2+}–O BC state.

Knowing that in c-Si interstitial substitutional exchange can occur with a moderate barrier ($\sim$0.5 eV),[18] we also examined the site exchange reaction between interstitial Ge and substitutional Si near the Si/SiO_2 interface, i.e., Si^{2+}–Ge–$Si^0 \rightarrow Si^{2+}$–Si–Ge^0. The exchange bears no significant change of total energy. This can be expected given the chemical similarity between Ge and Si. The kicked-out Si atom appears stabilized at the Si/SiO_2 interface in the form of Si^{2+}–O BC, Si^{4+}–O BC, or $\langle 111\rangle$-split, as demonstrated by a recent DFT study.[6] For neutral Si, the most favorable Si^{4+}–O BC and Si^{2+}–O BC states are energetically comparable, while slightly more favorable than the $\langle 111\rangle$-split state.[6] The interface states are predicted to be far more stable than the $\langle 110\rangle$-split state in bulk Si, while the interface Si^{4+}–O BC state appears as favorable as the Si^{4+}–O BC site in bulk a-SiO_2. In bulk a-SiO_2, as mentioned earlier, the Si^{4+}–O BC Si can further be converted to the FC state with an energy gain of as much as 1.8 eV. This suggests that Si interstitials (created by the Ge–Si site exchange reaction) would be preferentially incorporated into the a-SiO_2 network while creating O-vacancy-related defects. This hypothesis can be supported by the fact that most of the Si atoms emitted from the Si/SiO_2 interface during thermal oxidation will migrate into the SiO_2 part.[19]

Our calculation results clearly demonstrate that Ge atoms introduced into the Si/SiO_2 system will be segregated in the Si region, preferentially near the strained Si/SiO_2 interface, consistent with earlier experimental observations of Ge pile-up at the Si_xGe_{1-x}/SiO_2 interface.[20,21] Based on the results, as illustrated in Fig. 5, we attempt to propose a possible mechanism contributing to Ge nanoparticle formation in a Si-rich oxide matrix. First, Si-rich regions are formed to a certain degree by phase separation to Si and SiO_x ($x < 2$), as proposed for Si nanoparticle formation in the oxide matrix.[22] Second, interstitial Ge atoms migrate into the Si-rich regions, and undergo site exchange with substitutional Si atoms. Third, the kicked-out Si atoms migrate to O-rich regions, followed by incorporation into the oxide matrix while creating oxygen vacancies.[7] As the Si–SiO_x phase separation proceeds via oxygen out-diffusion from Si-rich regions,[22] Ge nanoparticles would also grow by the Ge–Si exchange reaction. Here, we should admit that the growth process of Ge nanocrystals appears so complex that its underlying mechanism is still a subject of debate. Nevertheless, we expect that the proposed mechanism based on the Si–Ge site exchange reaction will contribute partly to the formation of Ge nanocrystals embedded in the silica matrix.

Conclusion

In summary, we report the structure, energetics, bonding, and diffusion of Ge in the Si/SiO_2 system based on plane-wave basis, pseudopotential total energy calculations. Our results show that interstitial Ge is most stable at the Si^{4+}–O BC site in both α-quartz and a-SiO_2. The barrier for Ge diffusion is predicted to be 1.7 eV in α-quartz, and increases up to 2.5 eV in a-SiO_2 (which is more flexible and deformable). At the Si(001)/a-SiO_2 interface, the Si^{2+}–Si^0 BC site turns out to be the most favorable for neutral Ge. In addition, we find that a Ge interstitial would undergo thermally activated site exchange with a lattice Si atom in the Si part near the Si/SiO_2 interface. The kicked-out Si interstitial prefers to migrate and incorporate favorably into the a-SiO_2 part. Based on the results, we propose a possible mechanism contributing to Ge nanoparticle formation in a Si-rich oxide matrix, involving Si–Ge site exchange in the Si part along with Si–SiO_2 phase separation. The improved understanding will assist in uncovering complex mechanisms underlying the synthesis of Ge nanocrystals embedded in the silica matrix.

Acknowledgments

We acknowledge National Science Foundation (CAREER-CTS-0449373 and ECS-0304026) and Robert A. Welch Foundation (F-1535) for their financial support. We also thank the Texas Advanced Computing Center for use of their computing resources.

The University of Texas at Austin assisted in meeting the publication costs of this article.

References

1. W. K. Choi, V. Ho, V. Ng, Y. W. Ho, S. P. Ng, and W. K. Chim, *Appl. Phys. Lett.*, **86**, 143114 (2005).
2. I. D. Sharp, Q. Xu, D. O. Yi, C. W. Yuan, J. W. Beeman, K. M. Yu, J. W. Ager, D. C. Chrzan, and E. E. Haller, *J. Appl. Phys.*, **100**, 114317 (2006).
3. G. Taraschi, S. Saini, W. W. Fan, L. C. Kimerling, and E. A. Fitzgerald, *J. Appl. Phys.*, **93**, 9988 (2003).
4. P. F. Lee, X. B. Lu, J. Y. Dai, H. L. W. Chan, E. Jelenkovic, and K. Y. Tong, *Nanotechnology*, **17**, 1202 (2006).
5. V. Ho, M. S. Tay, C. H. Moey, L. W. Teo, W. K. Choi, W. K. Chim, C. L. Heng, and Y. Lei, *Microelectron. Eng.*, **66**, 33 (2003).
6. T. A. Kirichenko, D. Yu, S. K. Banerjee, and G. S. Hwang, *Phys. Rev. B*, **72**, 035345 (2005).
7. D. Yu, G. S. Hwang, T. A. Kirichenko, and S. K. Banerjee, *Phys. Rev. B*, **72**, 205204 (2005).
8. A. Brunet-Bruneau, D. Souche, S. Fisson, V. N. Van, G. Vuye, F. Abeles, and J. Rivory, *J. Vac. Sci. Technol. A*, **16**, 2281 (1998).
9. J. W. Y. Perdew, *Phys. Rev. B*, **45**, 13244 (1992).
10. G. Kresse and J. Furthmuller, *VASP the Guide*, Vienna University of Technology, Vienna, Austria (2001).
11. D. Vanderbilt, *Phys. Rev. B*, **41**, 7892 (1990).
12. H. J. Monkhorst and J. D. Pack, *Phys. Rev. B*, **13**, 5188 (1976).
13. G. Mills and H. Jonsson, *Phys. Rev. Lett.*, **72**, 1124 (1994).
14. G. Mills, H. Jonsson, and G. K. Schenter, *Surf. Sci.*, **324**, 305 (1995).
15. A. D. Becke and K. E. Edgecombe, *J. Chem. Phys.*, **92**, 5397 (1990).
16. *CRC Handbook of Physics and Chemistry*, 85th ed., D. R. Lide, Editor, CRC Press, Boca Raton, FL (2005).
17. E. S. Marstein, A. E. Gunnaes, U. Serincan, S. Jorgensen, A. Olsen, R. Turan, and T. G. Finstad, *Nucl. Instrum. Methods Phys. Res. B*, **207**, 424 (2003).
18. D. Caliste, P. Pochet, T. Deutsch, and F. Lancon, *Phys. Rev. B*, **75**, 125203 (2007).
19. K. Taniguchi, Y. Shibata, and C. Hamaguchi, *J. Appl. Phys.*, **65**, 2723 (1989).
20. P. E. Hellberg, S. L. Zhang, F. M. dHeurle, and C. S. Petersson, *J. Appl. Phys.*, **82**, 5773 (1997).
21. K. H. Heinig, B. Schmidt, A. Markwitz, R. Grotzschel, M. Strobel, and S. Oswald, *Nucl. Instrum. Methods Phys. Res. B*, **148**, 969 (1999).
22. D. C. Yu, S. H. Lee, and G. S. Hwang, *J. Appl. Phys.*, **102**, 084309 (2007).